

# DEHYDRATION CHARACTERISTICS OF TARO ROOT (*COLOCASIA ESCULENTA*) SLICES USING A REFRACTANCE WINDOW™ DRYER

A.A. Akinola<sup>1\*</sup>, E.O. Ejiogu<sup>2</sup>, O.O. Eleoranmo<sup>3</sup>

<sup>1,2,3</sup>Chemical & Petroleum Engineering Department, University of Lagos,  
Lagos, Nigeria.

Article History: Received 27.4.2019; Revised 3.12.2019; Accepted 3.12.2019

## ABSTRACT

*This report presents the dehydration characteristics of Taro (*Colocasia esculenta*) root slices dried at 65, 75, 85 and 95°C in a fabricated laboratory scale Refractance Window™ dryer; the Taro root slices were 3.0, 4.5 and 6.0 mm thick. Moisture content and water activity variation data were taken during the drying operation for the process conditions selected. For the process conditions studied, the times required to dehydrate the moisture content to 0.11 g-water/g-solid varied between 55 to 260 minutes. For a given slice thickness, the drying times to reach the 0.11 g-water/g-solid moisture content decreased as the drying temperature increased. Also, for a given drying temperature, the drying times required to reach the 0.11 g-water/g-solid moisture content increased with slice thickness. The effective moisture diffusivity varied from  $8.14 \times 10^{-8}$  to  $9.53 \times 10^{-7}$  m<sup>2</sup>/s for the process conditions studied.*

**KEYWORDS:** *Taro Roots; thin-layer drying models; drying curves; Refractance Window™ Dryer; water activity*

## 1.0 INTRODUCTION

Taro, (*Colocasia esculenta*), also known as cocoyam is a perennial crop, cultivated for human consumption of its roots. Taro roots are staple foods in Southeast Asia, Africa, India, China, the Caribbean and the Polynesian islands, although they are thought to be native to Southern India and Southeast Asia (Kolchaar, 2006). Taro roots provide about 110 calories per 100g of serving; they also have a high potassium content - 591mg per 100g of serving (USDA, 2018).

---

\*Corresponding Email: [aaakinola@unilag.edu.ng](mailto:aaakinola@unilag.edu.ng)

Taro roots processed into powdered form, are used to prepare many cuisines around the world (Hudgens and Trillo, 2003). The powder preparation process is labor intensive; it involves washing, peeling, slicing, sometimes pre-boiling and dehydrating. The Taro slices are then milled to a powder form. Sun-drying has traditionally been the dehydrating method (Lancaster et al., 1982). However, this method may take about 3 to 5 days. There is, therefore, a need to find a faster drying process producing suitably dry final products.

Presented in this study is the investigation into the Refractance Window™ drying method for drying taro root slices. The Refractance Window™ drying technique was patented by Magoon (1986) and developed by MCD Technology Inc., Tacoma, WA, USA.

Operated under atmospheric pressure and temperatures below 100°C (Nindo and Tang, 2007), the use of Refractance Window™ dryers are emerging as a promising low-cost drying method appropriate for dehydrating food and agro-products (Ochoa-Martinez et al., 2012). The growing use of the Refractance Window™ drying technology is due to the fact that the 3 modes of heat transfer are employed to dehydrate the food sample, conduction from the plastic sheet, thermal radiation from the hot water through the plastic sheet and convection at the top surface of food material (Ortiz-Jerez et al., 2015).

Many researchers have investigated the use of the Refractance Window™ dryer in dehydrating foods. Pumpkin purée was dried by Nindo et al. (2003) in a Refractance Window™ dryer to evaluate the energy efficiency and study the extent of the microbial reduction. The experiments indicated that the moisture content on a wet basis, reduced to 5% from 80% in less than 5 min. The results showed that Refractance Window™ dryer is energy efficient, and is effective in reducing microbial proliferation.

Abonyi et al., (2002), evaluated the ascorbic acid and color retention characteristics of strawberry and carrot purees dried using the Refractance Window™ drying and the freeze drying methods. Ascorbic acid retention of the strawberry purees (94.0%) after Refractance Window™ drying was comparable to 93.6% in freeze-drying. The colour of the Refractance Window™ dried carrot purees was akin to that of fresh puree. For Refractance Window™ dried strawberry purees, the color retention was similar to freeze-dried products.

The Refractance Window™ technique was used in drying purees and juices prepared from fruits, vegetables, and herb; Nindo and Tang (2007) observed that the purees and juices dried to about 4% moisture content within 3-5 minutes when the water temperature in the flumes was about 95 – 97°C.

Zotarelli et al., (2015), investigated the effect of process variables on the drying characteristics of mango pulp by Refractance Window™ drying. For process conditions in which the mango pulp thickness was 2, 3 and 5mm, water bath temperature of 75, 85 and 95°C, and the Mylar film was either transparent or painted; the radiation energy was higher with the transparent film than the black painted Mylar film. The change in colour values was higher with the oven-dried kiwifruits than the Refractance Window™ dried samples, and the drying rate increased with the water bath temperature.

Tontul and Topuz, (2017), investigated the effect of drying pomegranate leather, pestil, by microwave-assisted drying (MWD) and by the Refractance Window™ drying methods on some physicochemical properties. They concluded that the Refractance Window™ drying provided higher ascorbic acid and anthocyanin content, and lower content of 5-hydroxymethylfurfural, and the Refractance Window™ drying technique are the most promising processing methods for high-quality pestil production with a high content of bioactive compounds.

Akinola et al., (2018b) dehydrated 3.0mm thick ginger slices in a laboratory scale Refractance Window™ dryer; they indicated that the ginger root slices dried to a moisture content of 0.1g H<sub>2</sub>O/g solid on a dry basis in about 210 minutes.

To model dryers, and to perform the proper calculations for the design of dryers, knowledge of the characteristics of the dryer, and the product being dehydrated is required. This work presents the study of the effect of different process conditions on the drying curve of Taro roots slices using a Refractance Window™ dryer. The moisture diffusivity, of the dried Taro root slices, are estimated, the variation in the moisture content and the water activity of the Taro root slices are presented.

## 2.0 METHODS AND MATERIALS

### 2.1 Drying Apparatus

The dehydration of Taro (aka Cocoyam) root slices was performed on a fabricated laboratory scale Refractance Window™ dryer. The apparatus had similar components to those used by Akinola and Ezeorah (2018) and Ezeorah (2018). Figure 1 shows a schematic diagram of the drying apparatus. The drying apparatus consists of a rigid stainless steel shallow rectangular container, 1.0 meter in length, 0.5 meters wide, and 75 mm deep. The stainless steel container was filled with water, and it was covered with a transparent polyethylene terephthalate (PET) Mylar plastic film which was 0.15 mm thick. The PET Mylar plastic film covering was held in place with metal brackets and arranged so that the coverings lower surface was always in contact with the water. The water in the drying apparatus was heated using a 2.5 kW heater, which was controlled using a BAYITE BTC211 Digital Temperature Controller (Shenzhen Bayite Technology Co., Ltd., 2018). A hood covered the drying apparatus, and an extractor fan in the hood removed the moist air during operation; this was to ensure that the moist air does not inhibit the drying process.

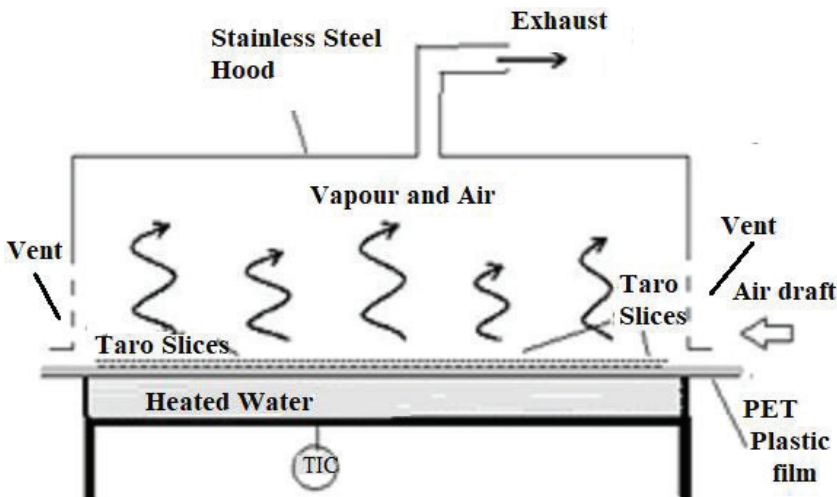


Figure 1 A Schematic Diagram of a Refractance Window Dryer (Akinola et al., 2018a)

## **2.2 Measurements**

The moisture content and weight of the cocoyam slices, both before and after the drying operation were measured using a Moisture Analyser (MB45, OHAUS, Parsippany, NJ, USA). The thickness of the cocoyam slices was determined using a digital Vernier calliper ( $\pm 0.02$  mm) (Mitutoyo, Waterbury, CT, US). Type K thermocouples (The Digi-Sense® Type K, Oakton Instruments, Vernon Hills, IL, USA) was used to measuring the temperature in the equipment to an accuracy of  $0.1^{\circ}\text{C}$ . The water activity of the dehydrated slices was determined water activity meter which had an accuracy of  $+0.02$  ( $P_{a_w}$  kit, Deacon Devices, Pullman, WA, USA).

## **2.3 Sample Preparation and Experimental Procedure**

Taro roots used in this study were bought from a local market. The roots have an oblong shape, and were between 7cm to 15cm in length, and had diameters between 2.5 and 5.0cm. The Taro roots tubers were cut into slices 3.0, 4.5 and 6.0mm thick, using a Mandolin slicer (SKU 1155700V2, OXO, Chambersburg, PA, USA), and then carefully cut into 2.54cm squares with a sharp knife. Thin slices were used because thicker slices take a relatively long time to dry (Azizi et al., 2017), which is a feature that is not desired. Also, the size range of Taro root slices selected for this study is within the 1.0 - 6.0mm slice sizes for most experiments done in the literature (Madamba et al., 1996; Azizi et al., 2017).

For 3.0, 4.5 and 6.0mm thick slice sizes, dehydration experiments were performed with water temperatures of  $65^{\circ}\text{C}$ ,  $75^{\circ}\text{C}$ ,  $85^{\circ}\text{C}$ , and  $95^{\circ}\text{C}$  in the Refractance Window™ dryer. Therefore, a total of 12 sets of experiments were performed. As indicated by Akinola et al. (2018a, 2018b), the upper-temperature limit of  $95^{\circ}\text{C}$  was selected to be slightly lower than the maximum possible operating temperature ( $100^{\circ}\text{C}$ ) for a Refractance Window™ dryer. The lower drying temperature of  $65^{\circ}\text{C}$  was chosen to avoid a relatively long drying time. The  $75^{\circ}\text{C}$  and  $85^{\circ}\text{C}$  temperatures were picked to enable a proper study of the drying kinetics within the lower and upper temperatures boundaries.

The initial moisture content of the Taro root slices, determined using the OHAUS Moisture Analyser (OHAUS Corporation, 2011), was 68% on a wet basis. A dozen sets of experiments were performed, each for a combination of a temperature and a slice thickness. The drier was started and allowed to attain

the desired temperature before loading of samples on the heated transparent polyethylene terephthalate (PET) Mylar plastic film. Approximately 700gm of Taro slices was loaded on the plastic film in a thin-layer. At 5-minute intervals, during the experiments, approximately 5gms 3 times of Taro slices were removed from the dryer, and their moisture content determined. All drying operations were performed 3 times.

## 2.4 Experimental Environment

Over the several days of experimentation, the ambient temperature in the laboratory, ranged from 29 to 31°C, while the humidity varied between 53 to 62%. During the drying operations, the surface of the dryer was exposed to ambient conditions with a draft of air of about 1 m/s over the drying surface. The draft of air was to ensure that the evaporating moisture did not inhibit the dehydration process. The relative humidity and temperature ranges were measured using a Thermo-Hygrometer Moisture Meter (Model RH700, Omega Engineering, Inc., Stamford, CT, USA).

## 2.5 Moisture Ratio Relationships

The moisture ratio after any given drying period was determined using Equation 1 (Sharifian et al., 2012; Toriki-Harchegani et al., 2016; Manzoor et al., 2017).

$$MR = \frac{MC_t - MC_e}{MC_i - MC_e} \quad (1)$$

Where

$MC_t$  is the moisture content of cassava after drying for time  $t$ ;

$MC_e$  is the equilibrium moisture content of dried cassava and

$MC_i$  is the initial moisture content of fresh cocoyam all in the unit of kg of water removed/kg of solids.

Many relationships known as the thin-layer drying models, exist between moisture ratio (MR) and the drying time,  $t$ . These thin-layer drying models are discussed extensively in literature (Erbay and Icier, 2010; Kucuk et al., 2014; Ezeorah, 2018). However, 9 common thin-layer drying models used in the dehydration of roots, corms, bulbs, fruits, and vegetables were used in this study are presented in Table 1.

**Table 1** Thin-layer drying models used for this study.

S/N	Model Names	Models	Reference
1.	Newton	$MR = \exp(-kt)$	(Ayensu, 1997)
2.	Page	$MR = \exp(-kt^n)$	(Page, 1949)
3.	Modified Henderson and Pabis	$MR = a \exp(-kt) + b \exp(-gt) + c \exp(-ht)$	(Karathanos, 1999)
4.	Logarithmic	$MR = a \exp(-kt) + c$	(Togrul and Pehlivan, 2003)
5.	Demir et al.	$MR = a \exp(-kt)^n + b$	(Demir et al., 2007)
6.	Verma et al.	$MR = a \exp(-kt) + (1-a) \exp(-gt)$	(Akpınar, 2010)
7.	Weibull	$MR = a - b \exp(-k_0 t^n)$	(Tzempelikos et al., 2014)
8.	Peleg	$MR = 1 - t/(a + bt)$	(da Silva et al., 2015)
9.	Haghi and Ghanadzadeh	$MR = a \exp(-bt^c) + dt^2 + et + f$	(Haghi and Ghanadzadeh, 2005)

Also, the relationship between moisture ratio (MR) and the effective moisture diffusivity, ( $D_{eff}$ ), as proposed by Crank (1975) for the Fick's second law of diffusion is shown in Equation 2.

$$MR = \frac{8}{\pi^2} \sum_{n=0}^{\infty} \frac{1}{(2n+1)^2} e^{-\left(\frac{(2n+1)^2 \pi^2 D_{eff} t}{4L^2}\right)} \quad (2)$$

where,

MR is the moisture ratio,

$D_{eff}$  ( $m^2s^{-1}$ ) is the effective moisture diffusivity,

$L$  (m) is the sample thickness and,

$t$  is the drying time (s).

However, for long drying periods, Eq. (3) can be simplified to only the first term of the series and written as,

$$MR = \frac{8}{\pi^2} e^{-\left(\frac{\pi^2 D_{eff} t}{4L^2}\right)} \quad (3)$$

## 2.6 Determination of the Effective Moisture Diffusivity

The relationship between moisture ratio (MR) and effective moisture diffusivity, ( $D_{eff}$ ), presented in equation 3 is used to estimate the moisture diffusivity. A linearized form of Equation 3 is given in Equation 4.

$$\ln(MR) = \ln\left(\frac{8}{\pi^2}\right) - \frac{\pi^2 D_{eff} t}{4L^2} \quad (4)$$

Using the moisture content dehydration data, a simple linear regression analysis between  $-\ln(MR)$  and drying time,  $t$ , gives a slope of  $k_d$  from which  $D_{eff}$  can be obtained according to the Equation 5.

$$k_d = \frac{\pi^2 D_{eff}}{4L^2} \quad (5)$$

## 2.7 Evaluation the Moisture Ratio and Drying Time Relationship

The thin-layer drying models are evaluated by fitting the experimental drying data to the models presented in Table 1. The thin-layer drying model that best describes the drying data of the cocoyam slices is the one which satisfies the following three statistical criteria. The criteria are that the coefficient of determination ( $R^2$ ), be closest to unity, the sum-of-square-error (SSE), and the root-mean-square-error (RMSE) be closest to zero. The method of estimating  $R^2$ , SSE and RMSE and the reason for them being to assert the best fit of relationships are discussed extensively in literature (Ogunnaike, 2011; Chail and Draxler, 2014; Johnson, 2017). This method of evaluation has been used in work done on drying characterization of agricultural food products (Ertekin and Yaldiz, 2004; Kabiru et al., 2013, Sanful et al., 2015; Akinola et al., 2016). The Matrix Laboratory software (MATLAB) was used to perform the statistical analysis (MathWorks, (2016).

## 2.8 Water Activity Measurement

During the drying process, variation in the moisture content and water activity data of the cocoyam slices was measured. The water activity of the cocoyam slices was measured using the  $P_{a_w}$ Kit. The  $P_{a_w}$ Kit is a Portable water activity meter developed by Deacon Devices Pullman, Washington, USA.  $P_{a_w}$ Kit determines water activity with an accuracy within  $\pm 0.02$ . Food and agro products with high water activity values are susceptible to microbial/fungal spoilage. Hence, the water activity of the dehydrating product was monitored during the drying process.



### 3.0 RESULTS AND DISCUSSION

#### 3.1 The Drying Curves

Plots of the variation of moisture ratio with time, for the different Taro root slice thicknesses, at 65, 75, 85, and 95°C are shown in Figures 2, 3, 4, and 5 respectively. The plots in Figures 2–5 show that for any given water temperature in the Refractance Window™ dryer, the moisture ratio of the slices decreased exponentially with time. Meanwhile, as the Taro slice thickness increased from 3.0 mm to 6.0 mm, an increase in drying time occurred. This is because, as the slice thickness increases, there is an increase in the amount of moisture that has to be removed from the slice. Therefore, the drying process is prolonged.

From the drying curves presented in Figures 2 to 5, the drying times required to dehydrate the Taro slices to 0.10g-water/g-solid increases with increasing slices thickness for a given temperature. Also, as the drying temperature increases, the drying times decreases for a given slice size; this is consistent with work done on yams and carrots (Akinola et al., 2016, Akinola et al., 2018a). Table 2 presents quantitative values of the drying times for different Taro slice sizes at different temperatures.

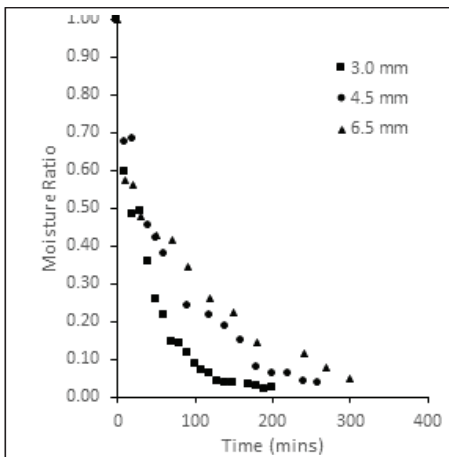


Figure 2 Drying curves for different Taro root slices at 65°C

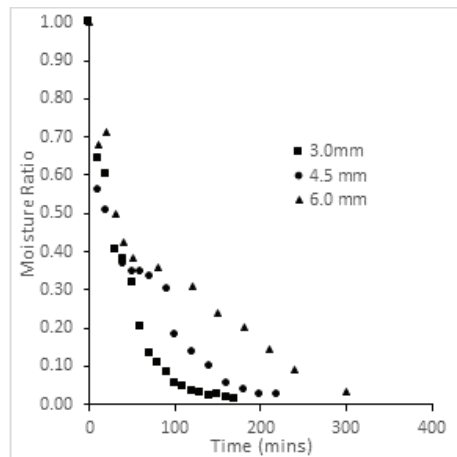


Figure 3 Drying curves for different Taro root slices at 75°C

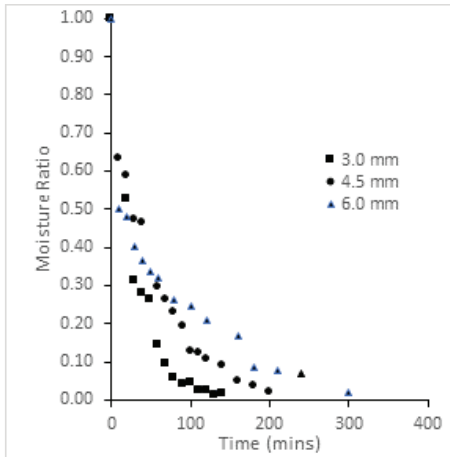


Figure 4 Drying curves for different Taro root slices at 85°C

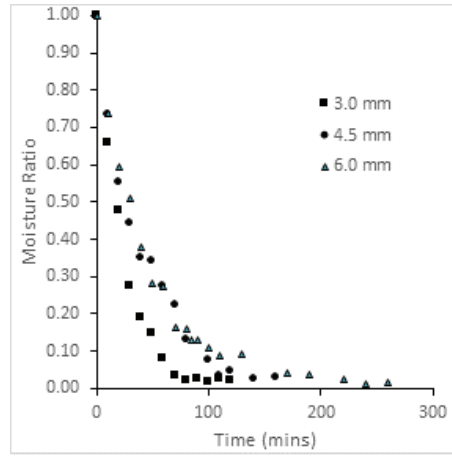


Figure 5 Drying curves for different Taro root slices at 95°C

Table 2 Drying Times for Different Taro Slice Sizes at Different Temperatures

Size	Temperature			
	65°C	75°C	85°C	95°C
3.0 mm	95 minutes	85 minutes	75 minutes	55 minutes
4.5 mm	175 minutes	145 minutes	120 minutes	85 minutes
6.0 mm	260 minutes	250 minutes	190 minutes	100 minutes

### 3.2 Moisture Ratio and Drying Time Relationship

The thin layer drying model that best describes the relationship between moisture ratio and drying time, the drying kinetics, was determined by fitting the experimental drying data to the models presented in Table 1. The thin-layer drying model that best describes the drying kinetics of the Taro slices is the one in which the following three criteria are satisfied. The criteria are: the coefficient of determination ( $R^2$ ) is to be closest to unity, the sum of square-error (SSE) and the root mean-square-error (RMSE) are closest to zero (Ertekin and Yaldiz, 2004; Kabiru et al., 2013, Sanful et al., 2015; Akinola et al., 2016, 2018b). The method of estimating  $R^2$ , SSE and RMSE are discussed extensively in literature (Ogunnaike, 2011; Johnson, 2017), and have been used in works on drying kinetics of agricultural food materials (Ertekin and Yaldiz, 2004; Kabiru et al., 2013, Sanful et al., 2015; Akinola et al., 2016). The Matrix Laboratory software (MATLAB) was used to perform the statistical analysis.

The results of the statistical analysis for fitting the thin-layer drying models are presented in Tables 3 – 5. For the 12 sets of experiments performed, all the 9 models were observed to fit the experimental data with a coefficient of variance  $R^2$ , greater than 0.96. However, the Haghi and Ghanadzadeh (2005) thin-layer drying model was found to fit because it had an  $R^2$  value closest to unity. The constants obtained for the Haghi and Ghanadzadeh model at different slice sizes and drying temperature are presented in Table 6.

### **3.3 Validation of Selected Models**

To establish that the Haghi and Ghanadzadeh (2005) thin-layer drying model best fits the drying kinetics, the relationship between the predicted (PMR) and experimental moisture ratio (EMR) values was determined. Table 7 shows that in all cases, the linear relationship had slopes close to unity and intercepts close to zero. Also, in all cases, the coefficient of variance ( $R^2$ ), was greater than 0.99 (Table 7). The implication is that there was no significant difference between the experimentally determined and the predicted moisture ratios for the process conditions considered, when modelling using the Haghi and Ghanadzadeh (2005) thin-layer drying model.

### **3.4 Estimating the Effective Moisture Diffusivity**

The effective moisture diffusivity,  $D_{eff}$ , was estimated using equation 2. The moisture content of the dehydrated taro slices was converted to moisture ratio (MR) using equation 1. By performing a simple linear regression between  $-\ln(MR)$  and the drying time for the process condition considered, the slope,  $k_d$ , is obtained, and the effective moisture diffusivity,  $D_{eff}$ , is estimated using equation 3. The linear relationship between MR, and drying time,  $t$ , is presented in Table 8. Table 8 also presents the correlation coefficients,  $R^2$ , obtained by performing simple linear regression, so is the effective moisture diffusivity,  $D_{eff}$ , at a given temperature. Table 8 shows that at a given temperature, the values of  $D_{eff}$  increase with increase in slice size.

Table 9 presents the effect of temperature on the effective moisture diffusivity,  $D_{eff}$ , at a given slice size. The Table shows that at a given slice size, the value  $D_{eff}$  increase with increase in drying temperature.

For comparing the results obtained, no documentation was found in the literature for the effective moisture diffusivity of Taro (cocoyam) slices in a Refractance Window™ dryer. However, the  $8.14 \times 10^{-08}$  to  $9.53 \times 10^{-07}$  m<sup>2</sup>/s effective moisture diffusivity values obtained in this study, is within the range of  $8.20 \times 10^{-14}$  to  $1.17 \times 10^{-05}$  m<sup>2</sup>/s values obtained for Moisture diffusivity of foods and agro-products in a review by Panagiotou et al., (2004).

### 3.5 Variation of Water Activity

The variation in moisture content and water activity,  $\alpha_w$ , is presented in Figure 6. The variation indicates that at a water activity of 0.5 the moisture content is about 0.1 g-water/g-solid. At a water activity,  $\alpha_w$ , of below 0.6, there is no possibility of microbial proliferation (LABCELL, 2017). The implications if that by dehydrating Taro slice to a moisture content of 0.10 g-water/g-solid microbial proliferation can be avoided.

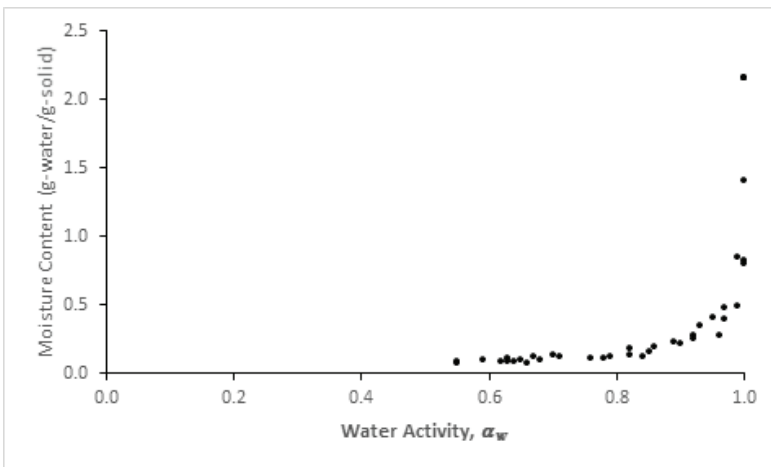


Figure 6 Variation in Moisture content with Water Activity

**Table 3** Results of Statistical Analysis For 3.0 mm Taro Slices at Different Temperatures

		3.0mm											
		65°C			75°C			85°C			95°C		
S/N	Model	SSE	R <sup>2</sup>	RMSE	SSE	R <sup>2</sup>	RMSE	SSE	R <sup>2</sup>	RMSE	SSE	R <sup>2</sup>	RMSE
1	Haghi and Ghanadzadeh Model	0.011	0.988	0.028	0.011	0.988	0.031	0.005	0.994	0.025	0.003	0.996	0.019
2	Verma et al Model	0.010	0.991	0.025	0.014	0.988	0.031	0.014	0.988	0.034	0.003	0.996	0.018
3	Diffusion Approach Model	0.010	0.991	0.025	0.014	0.988	0.031	0.014	0.988	0.034	0.003	0.996	0.018
4	Two-Term Model	0.010	0.990	0.025	0.014	0.987	0.032	0.014	0.987	0.035	0.003	0.996	0.019
5	Modified Handerson and Pabis Model	0.010	0.989	0.027	0.014	0.985	0.034	0.008	0.991	0.030	0.003	0.995	0.022
6	Page Model	0.018	0.985	0.032	0.019	0.985	0.034	0.018	0.986	0.037	0.003	0.997	0.017
7	Weibull Model	0.018	0.985	0.032	0.019	0.985	0.034	0.018	0.986	0.037	0.003	0.997	0.017
8	Two-Term Exponential Model	0.022	0.982	0.035	0.015	0.988	0.031	0.021	0.984	0.040	0.003	0.997	0.018
9	Modified Page Equation II Model	0.018	0.984	0.033	0.019	0.984	0.035	0.018	0.985	0.039	0.003	0.997	0.018

**Table 4** Results of Statistical Analysis For 4.5 mm Taro Slices at Different Temperatures

		4.5mm											
		65°C			75°C			85°C			95°C		
S/N	Model	SSE	R <sup>2</sup>	RMSE	SSE	R <sup>2</sup>	RMSE	SSE	R <sup>2</sup>	RMSE	SSE	R <sup>2</sup>	RMSE
1	Haghi and Ghanadzadeh Model	0.011	0.986	0.034	0.010	0.984	0.033	0.005	0.993	0.023	0.056	0.924	0.089
2	Verma et al Model	0.010	0.990	0.029	0.018	0.979	0.038	0.006	0.994	0.022	0.029	0.972	0.054
3	Diffusion Approach Model	0.010	0.990	0.029	0.018	0.979	0.038	0.006	0.994	0.022	0.029	0.972	0.054
4	Two-Term Model	0.010	0.989	0.030	0.018	0.977	0.040	0.006	0.993	0.022	0.029	0.969	0.057
5	Modified Handerson and Pabis Model	0.010	0.987	0.033	0.018	0.972	0.044	0.030	0.960	0.055	0.007	0.991	0.031
6	Page Model	0.015	0.986	0.034	0.039	0.956	0.055	0.016	0.984	0.034	0.034	0.971	0.055
7	Weibull Model	0.015	0.986	0.034	0.039	0.956	0.055	0.016	0.984	0.034	0.034	0.971	0.055
8	Two-Term Exponential Model	0.027	0.975	0.046	0.082	0.909	0.079	0.021	0.980	0.038	0.034	0.970	0.056
9	Modified Page Equation II Model	0.015	0.985	0.035	0.039	0.953	0.057	0.016	0.983	0.035	0.034	0.968	0.058

**Table 5** Results of Statistical Analysis For 6.0 mm Taro Slices at Different Temperatures

		6.0mm											
		65°C			75°C			85°C			95°C		
S/N	Model	SSE	R <sup>2</sup>	RMSE	SSE	R <sup>2</sup>	RMSE	SSE	R <sup>2</sup>	RMSE	SSE	R <sup>2</sup>	RMSE
1	Haghi and Ghanadzadeh Model	0.004	0.994	0.021	0.023	0.965	0.053	0.003	0.995	0.017	0.005	0.993	0.026
2	Verma et al Model	0.005	0.995	0.019	0.027	0.969	0.050	0.005	0.995	0.018	0.007	0.993	0.025
3	Diffusion Approach Model	0.005	0.995	0.019	0.027	0.969	0.050	0.005	0.995	0.018	0.007	0.993	0.025
4	Two-Term Model	0.005	0.994	0.020	0.027	0.966	0.052	0.005	0.994	0.019	0.007	0.993	0.026
5	Modified Handerson and Pabis Model	0.005	0.993	0.022	0.026	0.959	0.057	0.005	0.993	0.020	0.007	0.991	0.029
6	Page Model	0.029	0.971	0.046	0.032	0.967	0.051	0.021	0.977	0.038	0.006	0.994	0.023
7	Weibull Model	0.029	0.971	0.046	0.032	0.967	0.051	0.021	0.977	0.038	0.006	0.994	0.023
8	Two-Term Exponential Model	0.124	0.879	0.094	0.088	0.908	0.086	0.139	0.849	0.096	0.007	0.994	0.024
9	Modified Page Equation II Model	0.029	0.969	0.048	0.032	0.964	0.054	0.021	0.975	0.039	0.006	0.994	0.024

**Table 6** Evaluated Constants for the Haghi and Ghanadzadeh for Taro Drying at Different Temperature and Sizes

S/N	Parameters		Constant						
	Temperature (°C)	Slice Size (mm)	<i>a</i>	<i>b</i>	<i>c</i>	<i>d</i>	<i>e</i>	<i>f</i>	
1	65	3.0	9.56E-01	1.66E-01	4.27E-01	1.46E-05	-3.89E-03	4.24E-02	
		4.5	1.17E+00	8.23E-02	5.08E-01	2.80E-06	-1.06E-03	-1.73E-01	
		6.0	6.89E-01	5.84E-01	1.59E-01	2.97E-06	-2.30E-03	3.11E-01	
2	75	3.0	8.87E-01	1.22E-01	4.53E-01	2.74E-05	-6.59E-03	1.12E-01	
		4.5	4.08E-01	5.20E-01	8.80E-01	1.05E-05	-4.94E-03	5.94E-01	
		6.0	5.07E-01	7.34E-02	9.27E-01	1.88E-06	-2.00E-03	4.86E-01	
3	85	3.0	4.17E-01	3.10E-04	2.80E+00	3.84E-05	-9.36E-03	5.82E-01	
		4.5	2.11E+00	1.02E-01	1.62E-01	1.79E-05	-6.15E-03	-1.11E+00	
		6.0	8.30E-01	5.16E-01	2.09E-01	2.59E-06	-1.77E-03	1.70E-01	
4	95	3.0	1.52E+00	3.39E-02	9.36E-01	-1.27E-05	5.43E-03	-5.21E-01	
		4.5	1.43E+00	1.59E-01	1.25E-01	3.01E-05	-8.53E-03	-4.68E-01	
		6.0	1.81E+00	2.34E-02	8.84E-01	-1.09E-05	5.72E-03	-8.14E-01	

**Table 7** Experimental and predicted moisture Ratio at different temperatures

S/N	Temperature (°C)	Slice Size (mm)	Relationship	R <sup>2</sup>
1	65	3.0	PMR = 0.9906EMR + 0.0020	0.9909
		4.5	PMR = 0.9903EMR + 0.0034	0.9909
		6.0	PMR = 0.9960EMR + 0.0012	0.9960
2	75	3.0	PMR = 0.9915EMR + 0.0019	0.9914
		4.5	PMR = 0.9905EMR + 0.0029	0.9895
		6.0	PMR = 0.9783EMR + 0.0079	0.9782
3	85	3.0	PMR = 0.9961EMR + 0.0010	0.9960
		4.5	PMR = 0.9950EMR + 0.0017	0.9952
		6.0	PMR = 0.9968EMR + 0.0008	0.9966
4	95	3.0	PMR = 0.9974EMR + 0.0004	0.9978
		4.5	PMR = 0.9868EMR - 0.0273	0.9958
		6.0	PMR = 0.9955EMR + 0.0011	0.9956

**Table 8** Effect of Slice Size on the Effective Moisture Diffusivity at a Given Temperature.

SN	Drying Temperature	Slice Size	Relationship	R <sup>2</sup>	D <sub>eff</sub> (m <sup>2</sup> /s)
1	65°C	3.0 mm	-ln(MR65) = 0.0192t + 0.3674	0.9682	8.06E-07
		4.5 mm	-ln(MR65) = 0.0122t + 0.1854	0.9843	1.01E-07
		6.0 mm	-ln(MR65) = 0.0075t + 0.4147	0.9739	1.53E-07
2	75°C	3.0 mm	-ln(MR75) = 0.0255t + 0.1112	0.9841	8.14E-08
		4.5 mm	-ln(MR75) = 0.0163t + 0.1555	0.9717	1.28E-07
		6.0 mm	-ln(MR75) = 0.0090t + 0.2457	0.9583	1.48E-07
3	85°C	3.0 mm	-ln(MR85) = 0.0322t + 0.0160	0.9847	9.53E-07
		4.5 mm	-ln(MR85) = 0.0181t + 0.1143	0.9898	1.36E-07
		6.0 mm	-ln(MR85) = 0.0107t + 0.4151	0.9760	2.35E-07
4	95°C	3.0 mm	-ln(MR95) = 0.0368t + 0.2031	0.9296	1.23E-07
		4.5 mm	-ln(MR95) = 0.0246t - 0.0248	0.9817	1.56E-07
		6.0 mm	-ln(MR95) = 0.0160t + 0.3538	0.9663	2.78E-07

**Table 9** Effect of Temperature on the Effective Moisture Diffusivity at a Given Taro Slice Size

S/N	Slice Size	Drying Temperature	Relationship	R <sup>2</sup>	D <sub>eff</sub> (m <sup>2</sup> /s)
1	3.0 mm	65°C	-ln(MR65) = 0.0192t + 0.3674	0.9682	8.06E-07
		75°C	-ln(MR75) = 0.0255t + 0.1112	0.9841	8.14E-08
		85°C	-ln(MR85) = 0.0322t + 0.0160	0.9847	9.53E-07
		95°C	-ln(MR95) = 0.0368t + 0.2031	0.9296	1.23E-07
2	4.5 mm	65°C	-ln(MR65) = 0.0122t + 0.1854	0.9843	1.01E-07
		75°C	-ln(MR75) = 0.0163t + 0.1555	0.9717	1.28E-07
		85°C	-ln(MR85) = 0.0181t + 0.1143	0.9898	1.36E-07
		95°C	-ln(MR95) = 0.0246t - 0.0248	0.9817	1.56E-07
3	6.0 mm	65°C	-ln(MR65) = 0.0075t + 0.4147	0.9739	1.53E-07
		75°C	-ln(MR75) = 0.0090t + 0.2457	0.9583	1.48E-07
		85°C	-ln(MR85) = 0.0107t + 0.4151	0.9760	2.35E-07
		95°C	-ln(MR95) = 0.0160t + 0.3538	0.9663	2.78E-07

#### **4.0 CONCLUSION**

Slices of Taro roots, 3.0, 4.5 and 6.0 mm thick were dried in a Refractance Window™ dryer in which the dehydrating water temperature was 65, 75, 85, and 95°C. The Taro root slices were determined to have an initial moisture content of 2.16 g-water/g-solid, and they were dehydrated to a moisture ratio of about 0.1 g-water/g-solid. Variation in moisture content with dehydration time of the samples was recorded during the drying operations. Also, variation in water activity with dehydration time of the samples was recorded during the drying operations. The following conclusions can be made. Taro root slices 3.0 – 6.0 mm thick, dehydrated at 65 – 95°C in a Refractance Window™ dryer, can be dried to about 0.1 g-water/g-solid in about 55 to 260 minutes. The moisture diffusivity during dehydration under these process conditions varied between  $8.14 \times 10^{-08}$  and  $9.53 \times 10^{-07}$  m<sup>2</sup>s<sup>-1</sup>. At a moisture content of about 0.1 g-water/g-solid the water activity of Taro root slices water about 0.5. At a 0.5 water activity value, there can be no microbial proliferation within the root slices.

The drying curve is an important characteristic used in the design and modelling of dryers in the food industry. The water activity is also essential to know what level of dehydration is required to stop microbial proliferation. As limited literature was found on the drying characteristics for Taro roots in a Refractance Window™ dryer, this work presents these characteristics, and they will be useful for designing, modeling and operating such equipment.

#### **ACKNOWLEDGEMENT**

The authors are grateful to the Chemical and Petroleum Engineering Department, University of Lagos, Lagos, Nigeria for allowing them to use the laboratories and also, for the financial support provided by the Tertiary Education Trust Fund (TETFund), Nigeria under Grant CRC/TETFUND/NO.2018/04.

## REFERENCES

- Abonyi, B. I., Feng, H., Tang, J., Edwards, C. G., Chew, B. P., Mattinson, D. S., & Fellman, J. K., (2002), Quality retention in strawberry and carrot purees dried with Refractance Window™ System. *Journal of Food Science*, 67(3), 1051-1056. <https://doi.org/10.1111/j.1365-2621.2002.tb09452.x>
- Akinola, A. A. and Ezeorah, S. N., (2018), Dehydration Kinetics of Cassava, Yam and Potato Slices Using a Refractance Window™ Dryer, *FUOYE Journal of Engineering and Technology*, Vol 3, No. 2 (2018) pages 88 -92
- Akinola, A. A., Ayo, D. B. and Ezeorah, S. N., (2018a), Temperature Dependence of the Effective Moisture Diffusivity of Yam (*Dioscorea rotundata*) Slices Dried Using a Refractance Window™, *The Journal of the Association of Professional Engineers of Trinidad and Tobago*, ISSN 1000 7924,.46(1)
- Akinola, A. A., Azeta, O., & Ezeorah, S. N., (2018b). Evaluation of the Dehydration Characteristics of Ginger (*Zingiber Officinale*) Root Slices Using Refractance Window Drying Technology. *FUOYE Journal of Engineering and Technology*, 3(1).
- Akinola, A. A., Malomo, T. O. and Ezeorah, S. N., (2016), “Dehydration Characterisation of Carrot (*Daucus Carota*) Slices Dried Using the Refractance Window™ Drying Technique”, *Zimbabwe Journal of Science and Technology*, 11, 28-37
- Akpınar, E. K., (2010), Drying of Mint Leaves in a Solar Dryer and Under Open Sun: Modelling, Performance Analyses, *Energy Conversion and Management*, 51(12), 2407-2418. DOI: 10.1016/j.enconman.2010.05.005.
- Ayensu, A., (1997), Dehydration of Food Crops Using a Solar Dryer with Convective Heat Flow, *Solar Energy*, 59(4-6), 121-126. [https://doi.org/10.1016/S0038-092X\(96\)00130-2](https://doi.org/10.1016/S0038-092X(96)00130-2)
- Azizi, D., Jafari, S. M., Mirzaei, H., & Dehnad, D., (2017), The Influence of Refractance Window Drying on Qualitative Properties of Kiwifruit Slices, *International Journal of Food Engineering*, 13(2). <https://doi.org/10.1515/ijfe-2016-0201>
- Chail, T. and Draxler R. R., (2014), Root Mean Square Error (RMSE) or Mean Absolute Error (MAE)? – Arguments Against Avoiding RMSE in the Literature, *Geosciences Model Development*, 7, 1247–1250. <https://doi.org/10.5194/gmd-7-1247-2014>
- Crank, J., (1975), *The Mathematics of Diffusion*, 2<sup>nd</sup> ed., Oxford University Press, Oxford.



- da Silva, W. P., Rodrigues, A. F., de Silva, C. M. D., de Castro, D. S., & Gomes, J. P., (2015), Comparison Between Continuous and Intermittent Drying of Whole Bananas Using Empirical and Diffusion Models to Describe the Processes, *Journal of Food Engineering*, 166, 230-236. <https://doi.org/10.1016/j.jfoodeng.2015.06.018>
- Demir, V., Gunhan, T., and Yagcioglu, A. K. (2007). Mathematical Modelling of Convection Drying of Green Table Olives, *Biosystems Eng.*, 98, 47-53. <https://doi.org/10.1016/j.biosystemseng.2007.06.011>
- Erbay, Z., & Icier, F., (2010), A Review of Thin Layer Drying of Foods: Theory, Modeling, and Experimental Results, *Critical Reviews in Food Science and Nutrition*, 50(5), 441-464. <https://doi.org/10.1080/10408390802437063>
- Ertekin, C. and Yaldiz, O., (2004), Drying of Eggplant and Selection of a Suitable Thin Layer Drying Model, *Journal of Food Engineering*, 63(3), 349-359. <https://doi.org/10.1016/j.jfoodeng.2003.08.007>
- Ezeorah, S. N., (2018), *Evaluation of Refractance Window™ Drying technology for Yam Dehydration*, M.Sc., Research Report, Department Chemical and Petroleum Engineering, Lagos, Nigeria.
- Haghi, A. K. and Ghanadzadeh, H., (2005), A Study of Thermal Drying Process, *Indian Journal of Chemical Technology*, 12(1), 654-663.
- Hudgens, J. and Trillo, R., (2003), *The Rough Guide to West Africa*, Rough Guides (p. 1012). ISBN 1-843-53118-6.
- Johnson, R. A., (2017), *Miller and Freund's Probability and Statistics for Engineers*. Pearson Education © 2017. ISBN 10: 1-292-17601-6, ISBN 13: 978-1-292-17601-7
- Kabiru, A. A., Joshua, A. A. and Raji, A. O., (2013), Effect of Slice Thickness and Temperature on the Drying Kinetics of Mango (*Mangifera Indica*), *International Journal of Research and Review in Applied Sciences*, 15(1), 41-50.
- Karathanos, V.T., (1999), Determination of Water Content of Dried Fruits by Drying Kinetics, *Journal of Food Engineering*, 39(4), 337-344. [https://doi.org/10.1016/S0260-8774\(98\)00132-0](https://doi.org/10.1016/S0260-8774(98)00132-0)
- Kolchaar, K., (2006), *Economic Botany in the Tropics*, Macmillan India
- Kucuk, H., Midilli, A., Kilic, A., & Dincer, I. (2014). A Review on Thin-Layer Drying-Curve Equations. *Drying Technology*, 32(7), 757-773. <https://doi.org/10.1080/07373937.2013.873047>

- LABCELL Ltd, (2018), *Water Activity and Growth of Microorganisms in Food*, Labcell Ltd., Four Marks, Alton, Hampshire. GU34 5PZ
- Lancaster, P. A., Ingram, J. S., Lim, M. Y., & Coursey, D. G., (1982), Traditional Cassava-Based Foods: Survey of Processing Techniques, *Economic Botany*, 36(1), 12-45 <https://doi.org/10.1007/BF02858697>
- Madamba, P. S., Driscoll, R. H., & Buckle, K. A. (1996). The Thin-Layer Drying Characteristics of Garlic Slices. *Journal of Food Engineering*, 29(1), 75-97. [https://doi.org/10.1016/0260-8774\(95\)00062-3](https://doi.org/10.1016/0260-8774(95)00062-3)
- Magoon, R. E., (1986), *Method and Apparatus for Drying Fruit Pulp and the Like*. US Patent 4,631,837.
- Manzoor, M., Shukla, R. N., Mishra, A. A., Fatima, A., & Nayik, G. A., (2017), Osmotic Dehydration Characteristics of Pumpkin Slices using Ternary Osmotic Solution of Sucrose and Sodium Chloride. *Journal of Food Processing Technology*, 8(669), 2. <https://doi.org/10.4172/2157-7110.1000669>
- MathWorks, (2016). *MATLAB and Statistics Toolbox Release 2016b*, The MathWorks, Inc., Natick, Massachusetts, United States.
- Mitutoyo Corporation, (2014), *Quick Guide to Precision Measuring Instrument*, 20-1, Sakado 1 Chrome, Takatsu-ku, Kawasaki-shi, Kanagawa 213-8533, Japan
- Nindo, C., Sun, T., Wang, S. W., Tang, J., & Powers, J. R. (2003). Evaluation of drying technologies for retention of physical quality and antioxidants in asparagus (*Asparagus officinalis*, L.). *LWT-Food Science and Technology*, 36(5), 507-516. [https://doi.org/10.1016/S0023-6438\(03\)00046-X](https://doi.org/10.1016/S0023-6438(03)00046-X)
- Nindo C. I., Tang J., (2007), Refractance Window Dehydration Technology: A Novel Contact Drying Method. *Drying Technology* 25(1):37-48 <https://doi.org/10.1080/07373930601152673>
- Ochoa-Martínez, C. I., Quintero, P. T., Ayala, A. A., & Ortiz, M. J., (2012), Drying characteristics of Mango Slices Using the Refractance Window™ Technique. *Journal of Food Engineering*, 109(1), 69-75. 2002 Researchers <https://doi.org/10.1016/j.jfoodeng.2011.09.032>
- Ogunnaike, B. A., (2011), *Random Phenomena: Fundamentals of Probability and Statistics for Engineers*. CRC Press.

- OHAUS Corporation, (2011), *Instruction Manual MB45 Moisture Analyzer*, OHAUS Corporation, 7 Campus Drive, Suite 310, Parsippany, NJ 07054 USA.
- Ortiz-Jerez, M. J., Gulati, T., Datta, A. K., & Ochoa-Martínez, C. I., (2015), Quantitative understanding of refractance window™ Drying. *Food and Bioprocess Technology*, 95, 237-253. <https://doi.org/10.1016/j.fbp.2015.05.010>
- Page G. E., (1949), *Factors Influencing the Maximum Rates of Air Drying of Shelled Corn in Thin Layer*, M.Sc. Thesis, Purdue University, Lafayette, IN, USA.
- Panagiotou, N. M., Krokida, M. K., Maroulis, Z. B. and Saravacos, G. D., (2004), Moisture Diffusivity: Literature Data Compilation for Foodstuffs. *International Journal of Food Properties*, 7(2), 273-299. <https://doi.org/10.1081/JFP-120030038>
- Sanful, R. E., Addo, A., Oduro, I, Ellis, W. O., (2015), Air Drying Characteristics of Aerial Yam (*Dioscorea bulbifera*), *Scholars Journal of Engineering and Technology* (SJET), 2015; 3(8), 693-700.
- Sharifian, F., Motlagh, A. M., Nikbakht, A. M., (2012), Pulsed Microwave Drying Kinetics of Fig Fruit ('*Ficus carica*'L.). *Australian Journal of Crop Science*, 6(10), 1441.
- Shenzhen Bayite Technology Co., Ltd., (2018), *BAYITE BTC211 Digital Temperature Controller Manual*, Retrieved January 27, 2018 from <https://images-na.ssl-images-amazon.com/images/I/91SaoMRr+8L.pdf>.
- Togrul, I. T. and Pehlivan, D., (2003), Modelling of Drying Kinetics of Single Apricot, *Journal of Food Engineering*, 58(1), 23-32. [https://doi.org/10.1016/S0260-8774\(02\)00329-1](https://doi.org/10.1016/S0260-8774(02)00329-1).
- Tontul, I., & Topuz, A., (2017), Effects of Different Drying Methods on the Physicochemical Properties of Pomegranate Leather (Pestil). *LWT-Food Science and Technology*, 80, 294-303. <https://doi.org/10.1016/j.lwt.2017.02.035>.
- Torki-Harchegani, M., Ghasemi-Varnamkhasti, M., Ghanbarian, D., Sadeghi, M., & Tohidi, M. (2016). Dehydration Characteristics and Mathematical Modelling of Lemon Slices Drying Undergoing Oven Treatment, *Heat and Mass Transfer*, 52(2), 281-289. <https://doi.org/10.1007/s00231-015-1546-y>.
- Tzempelikos, D. A., Vouros, A. P., Bardakas, A. V., Filios, A. E., & Margaritis, D. P., (2014), Case Studies on the Effect of the Air Drying Conditions on the Convective Drying of Quinces. *Case Studies in Thermal Engineering*, 3, 79-85. <https://doi.org/10.1016/j.csite.2014.05.001>.

United States USDA Department of Agriculture, (2018), *Agricultural Research Service USDA Food Composition Databases*, Retrieved August 01, 2018, from <https://ndb.nal.usda.gov/ndb/foods/show/11518?fgcd=&manu=&format=&count=&max=25&offset=&sort=default&order=asc&qlookup=Taro%2C+raw&ds=&qt=&qp=&qa=&qn=&q=&ing=>

Zotarelli, M. F., Carciofi, B. A. M., & Laurindo, J. B., (2015), Effect of Process Variables on the Drying Rate of Mango Pulp by Refractance Window. *Food Research International*, 69, 410-417 <https://doi.org/10.1016/j.foodres.2015.01.013>.